

Elsevier Editorial System(tm) for Thin Solid Films  
Manuscript Draft

Manuscript Number: TSF-D-12-03058R2

Title: Influence of annealing on polymeric precursor derived ZnO thin films on sapphire

Article Type: Full Length

Section/Category: E. Electronics, Optics, and Opto-electronics

Keywords: ZnO; thin films; polymeric precursor; annealing; ZnAl<sub>2</sub>O<sub>4</sub>

Corresponding Author: Dr. Uma Choppali, Ph.D.

Corresponding Author's Institution: Collin College

First Author: Uma Choppali, Ph.D

Order of Authors: Uma Choppali, Ph.D; Elias Kougianos, Ph.D.; Saraju P Mohanty, Ph.D.; Brian P Gorman, Ph.D.

Abstract: Zinc oxide (ZnO) thin films on c-sapphire substrates were synthesized by spin-coating aqueous polymeric precursors. The effects of annealing at 1000°C on crystallinity, surface morphology, and optical properties of ZnO thin films, with varying thicknesses, were studied. Single-layered ZnO thin films are polycrystalline with wurtzite structure and preferentially oriented along the (002) plane. X-ray diffraction pattern also reveal the presence of spinel zinc aluminate (ZnAl<sub>2</sub>O<sub>4</sub>) peaks. ZnO films have highly faceted granular morphology. Multilayered ZnO films, annealed twice at 1000°C, do not exhibit any ZnO peaks and only ZnAl<sub>2</sub>O<sub>4</sub> peaks. Moreover, the surface morphology was smooth with ridges. These films do not exhibit the band gap or ultra-violet emission photoluminescence characteristics of ZnO. On annealing, there is an interfacial reaction between ZnO and sapphire resulting in ZnAl<sub>2</sub>O<sub>4</sub>.

# **Influence of annealing on polymeric precursor derived ZnO thin films on sapphire**

*Uma Choppali<sup>a\*1</sup>, Elias Kougianos<sup>b</sup>, Saraju P. Mohanty<sup>b</sup>, and Brian P. Gorman<sup>2</sup>*

<sup>a</sup>Department of Materials Science and Engineering,  
University of North Texas, Denton, TX 76203, USA

<sup>b</sup>NanoSystem Design Laboratory (NSDL),  
University of North Texas, Denton, TX 76203, USA

<sup>1</sup>Department of Mathematics and Science,  
Collin College, Frisco, TX 75035, USA

<sup>2</sup>Colorado Center for Advanced Ceramics, Dept. of Metallurgical and Materials  
Engineering, Colorado School of Mines, Golden, CO 80401, USA.

Email-ID: [umachoppali@gmail.com](mailto:umachoppali@gmail.com)

Telephone: +1-940-231-0041

Fax: +1-940-565-2799

## **Abstract**

Zinc oxide (ZnO) thin films on c-sapphire substrates were synthesized by spin-coating aqueous polymeric precursors. The effects of annealing at 1000°C on crystallinity, surface morphology, and optical properties of ZnO thin films, with varying thicknesses, were studied. Single-layered ZnO thin films are polycrystalline with wurtzite structure and preferentially oriented along the (002) plane. **X-ray diffraction pattern** also reveal the presence of spinel **zinc aluminate** ( $\text{ZnAl}_2\text{O}_4$ ) peaks. ZnO films have highly faceted granular morphology. Multilayered ZnO films, annealed twice at 1000°C, do not exhibit any ZnO peaks and only  $\text{ZnAl}_2\text{O}_4$  peaks. Moreover, the surface morphology was smooth with ridges. These films do not exhibit the band gap or **ultra-violet** emission photoluminescence characteristics of ZnO. On annealing, there is an interfacial reaction between ZnO and sapphire resulting in  $\text{ZnAl}_2\text{O}_4$ .

Key words: ZnO, thin films, polymeric precursor, annealing,  $\text{ZnAl}_2\text{O}_4$

## 1. Introduction

Preferential orientation of zinc oxide (ZnO) thin films has technologically important applications as transparent electrodes of solar cells [1, 2], light emitting diodes [3, 4], and thin film transistors [5] because of their unique physical properties. ZnO is a direct wide band gap semiconductor with a band gap of 3.3 eV and high exciton binding energy (60 meV) at room temperature. Although there is a large lattice mismatch between ZnO and sapphire, textured ZnO thin films have been deposited on sapphire substrates due to their similar crystal structure. ZnO thin films on sapphire have been synthesized by different deposition methods including magnetron sputtering [6], atomic layer epitaxy [7], pulsed laser deposition [8], sol-gel [9], chemical solution deposition [10], and the Pechini process [11].

Prior research has been performed to study the effects of post-annealing on deposition and growth of ZnO films. The authors have annealed ZnO thin films at 800°C in N<sub>2</sub> atmosphere and studied the structural and optical properties of ZnO films [6]. It has been reported [12] that properties of ZnO films depend not only on annealing during the growth process but also on post-deposition annealing. Xue and his group [13] studied effects of post-annealing up to 950°C on the optical constants of ZnO films prepared by the sol-gel method. In [11, 14] the authors have annealed polymeric precursor derived ZnO thin films from 400°C to 1000°C and have studied their morphology and optical properties.

In this paper, the effect of high temperature annealing on multilayered spin-coated ZnO thin films on c-sapphire substrates is presented. Samples were prepared by annealing at 1000°C and also by spin-coating five layers of ZnO followed by annealing

again at 1000°C. **X-ray diffraction (XRD) and field emission scanning electron microscopy (FESEM)** characterization techniques were used to study the crystallinity and surface morphology of these two types of samples. Optical properties of the ZnO films were studied by **Ultra-Violet (UV)**-transmittance and photoluminescence (PL).

## **2. Experimental Methods**

### *2.1 Preparation of ZnO thin films*

Polymeric precursors were synthesized by the Pechini process using ethylene glycol and citric acid as the chelating agents [11]. The acquired chemicals were of analytical grades and were used as-received without further purification. In this process, citric acid was dissolved in 50 ml of deionized and filtered water (resistivity = 18.2MΩ). To this solution, 0.1 mole of zinc nitrate ( $Zn(NO_3)_2$ ), 0.9 mole of ethylene glycol, and 0.1 mole of nitric acid were added, followed by a large amount of deionized water. The solution was constantly stirred and heated for 10 hours at 70°C until the resulting solution was clear and precipitate free. Fig. 1 shows the preparation of polymeric precursors and ZnO thin films. The polymeric precursors were spin-coated (CEE Model 100CB, Brewer Science Inc., Rolla, MO) on c-axis sapphire substrates (Crystal systems Inc. Salem, MA) at 4000 rpm for 30 seconds, after cleaning the substrates by heating them in air at 900°C for 1 hour. After spin-coating, the films were cured on a hot plate at 70°C for 1 hour, followed by pre-heating at 300°C for 30 min. after which the films were annealed in an ambient furnace at a rate of 5°C/min at 1000°C for a hold time of 10 minutes, which is referred as Sample-1. After cooling down to room temperature, the precursors are again spin-coated on few samples and the as-deposited films are cured and pre-heated at 300°C

to remove the excess water. These steps were repeated five times, after which the films were annealed at 1000°C for 10 minutes, which will be referred to as Sample-2.

## 2.2 Characterization of ZnO thin films

X-ray diffraction patterns were obtained using Cu-K $\alpha$  radiation (40 kV and 44 mA) in grazing incidence in the range of 5° to 75° , in-plane ( $2\theta_\chi/\phi$ ), and  $\phi$  modes (Rigaku Ultima III model, Rigaku Corp., Tokyo, Japan). The surface morphology of the annealed thin films was characterized by field emission scanning electron microscopy, FESEM (Nova 200 NanoLab, FEI Co., Hillsboro, OR). The optical transparency of the annealed thin films was determined in transmission mode at normal incidence using a Variable Angle Spectroscopic Ellipsometer (VASE, J. A. Woollam, Inc., Lincoln, NE) without backside correction. Room temperature photoluminescence (PL) spectra were acquired using a scanning spectrofluorometer (Model QM-4, Photon Technology International Inc., Birmingham, NJ) with 340 nm as excitation wavelength using a Xenon lamp.

## 3. Results and Discussion

Grazing incidence X-ray diffraction (GIXRD) **pattern** of annealed ZnO thin films on sapphire substrates at 1000°C are shown in Fig. 2. Results show that Sample-1, which is single-layer annealed ZnO thin films, is polycrystalline with wurtzite structure (space group P6<sub>3</sub>mc). The diffraction peaks can be indexed to hexagonal ZnO (JCPDS No. 36-1451) with peaks along the (100), (002), and (101) planes. Besides these ZnO peaks, few low intense peaks of cubic spinel zinc aluminate, ZnAl<sub>2</sub>O<sub>4</sub> (JCPDS No. 05-

0669) were observed, which are assigned as (220), (311), (511), and (440) planes. **Results also show** that the ZnO films are preferentially oriented along the (002) plane. GIXRD **pattern** of Sample-2 show only peaks assigned to ZnAl<sub>2</sub>O<sub>4</sub>, such as (111), (220), (311), (511), and (440). No ZnO peaks were observed. Formation of ZnAl<sub>2</sub>O<sub>4</sub> may be due to an interfacial reaction between the ZnO film and the sapphire substrate on annealing at 1000°C [15]. On twice annealing at 1000°C, the five layers of ZnO films reacted completely with the sapphire substrate leading to more intense ZnAl<sub>2</sub>O<sub>4</sub> peaks. Preferential orientation is calculated from the intensity ratios of the (002) diffraction peak to the intensities of other strong (100) and (101) diffraction peaks and was found to be 2.57 for Sample-1 [11].

In-plane ( $2\theta_\gamma/\phi$ ) measurements were performed on the Sample-1 and Sample-2 ZnO thin films, as shown in Fig. 3. The **XRD pattern** for Sample-1 shows that the intensity of the (100) and (101) diffraction peaks is relatively stronger than the (002) peak. This data also confirms that all grains are aligned along the [001] basal planes of the ZnO thin film. The in-plane **pattern** of Sample-2 does not exhibit any ZnO diffraction peaks. Moreover, the diffraction peaks indexed to ZnAl<sub>2</sub>O<sub>4</sub> do not show any texturing. Fig. 4 shows XRD  $\phi$ -scans of the {101} family of planes for Sample-1, performed at an incident angle of 0.45° with the detector fixed at 36.25°. The  $\phi$ -scans display at least two sets of six peaks separated by 60°. This result indicates hexagonal symmetry confirming strong texturing with multiple orientations of the ZnO grains.

The surface morphology of the ZnO films depended strongly on the annealing temperature as analyzed by FESEM. Fig. 5 shows FESEM micrographs of Sample-1 and Sample-2 illustrating the effect of annealing on morphology. These micrographs

demonstrate that the morphology of the particles changes from highly faceted islands of ZnO in Sample-1 to continuous thin film of ZnAl<sub>2</sub>O<sub>4</sub> with few ridges in Sample-2. High magnification micrographs of Sample-1 reveal that the ZnO particles are polyhedral and faceted with a variation in shape and size, also observed in [8]. Particles, with sizes between 60-90 nm, are hemispherical, whereas larger ones, in the size range of 150 – 350 nm are flat hexagonal in shape, promoting further grain growth atop of these grains. ZnO grains agglomerate at 1000°C resulting in unoccupied space around them. SEM micrographs of Sample-2 indicate that the surface of the ZnAl<sub>2</sub>O<sub>4</sub> film is uniform with ridge-like structure, similar to the results reported in [15].

Thickness of the Sample-1 and Sample-2 was measured from Focused Ion Beam (FIB) cross-section micrographs using FEI Co. software. At 900°C, ZnO films were 160 nm thick, measured from FIB cross-section [11]. Micrographs of Sample-1 show that the ZnO films are not uniform. Thickness of ZnO varies from 180 nm to 290 nm across the cross-section, confirming that the ZnO is agglomerated, as shown in Fig 6a. An FIB cross-section micrograph of Sample-2, shown in Fig. 6b, does not show a clear demarcation between the ZnO film and sapphire substrate, due to grain boundary diffusion.

UV-Vis transmission spectra of both samples, in the wavelength range 260–800 nm, are shown in Fig. 6. Sample-1, ZnO thin film, annealed at 1000°C shows transmittance, in arbitrary units (**arb.units**), of less than 50% in the visible region that may be attributed to increase in grain size resulting in an increase in scattering of light [16]. Sample-1 illustrates sharply decreasing transmittance in the UV region because of the onset of absorption with a band edge at 376 nm corresponding to ZnO. Sample-2 does

not exhibit any band edge at 376 nm confirming that ZnO is absent. ZnAl<sub>2</sub>O<sub>4</sub> is also a wide band gap semiconductor with near UV band edge at 323 nm (3.8 eV). However, the band edge of ZnAl<sub>2</sub>O<sub>4</sub> is not observed in Sample-2. It has been reported that the size of nanoparticles affects the optical properties leading to a blue shift from the bulk band gap value. In [17, 18] the authors have reported synthesized ZnAl<sub>2</sub>O<sub>4</sub> nanoparticles having a band gap in the range of 4.02 to 4.7 eV. Based on this, it may be deduced that the ZnAl<sub>2</sub>O<sub>4</sub> particles of Sample-2 may have blue-shifted the band gap energy value.

Room temperature PL spectra of Sample-1 and Sample-2 are shown in Fig. 7. The PL spectrum of Sample-1 shows a broad UV emission peak, which is a near band edge emission attributed to the radiative annihilation of excitons as ZnO. No other emissions related to structural defects in ZnO are observed suggesting high crystallinity of Sample-1. No PL spectra are observed in Sample-2 implying that ZnO is absent.

Deposition of thin films involves the processes of nuclei formation, growth, and coalescence of grains. During annealing at 1000°C, the ZnO grains gain sufficient thermal energy leading to coalescence of the grains. Large hexagonal ZnO grains must have coalesced due to Ostwald ripening leading to abnormal grain growth. FESEM results of Sample-1 also reveal some necks connecting the grains showing sintering also occurred. Hence, FESEM results of Sample-1 show that sintering and Ostwald ripening occur simultaneously leading to grain growth. Moreover, flattened ZnO grains were also observed, which may be due to evaporation of ZnO nanoparticles [19]. There is also grain boundary diffusion of zinc ions during Ostwald ripening [19] into the sapphire substrate, resulting in an interfacial ZnAl<sub>2</sub>O<sub>4</sub> layer.

In this work, single-layered ZnO thin films deposited on sapphire are preferentially oriented along the (002) plane with the growth direction along [001]. After annealing, XRD results of Sample-1 reveal the presence of ZnAl<sub>2</sub>O<sub>4</sub> acting as an interfacial layer leading to marked texturing in ZnO films. These ZnO films have topotactical relationship of (001)<sub>ZnO</sub> // (111)<sub>spinel</sub> // (001)<sub>sapphire</sub> [10, 20]. During the thermal annealing at 1000°C, the zinc cations diffused into the Al<sub>2</sub>O<sub>3</sub> lattice and the oxygen sublattice of Al<sub>2</sub>O<sub>3</sub> changes from hexagonal-closed packed structure to face-centered-cubic spinel ZnAl<sub>2</sub>O<sub>4</sub> [20, 21]. The close packed planes (111) of ZnAl<sub>2</sub>O<sub>4</sub> grow parallel to the (001) ZnO and (0001) planes of c-sapphire substrate.

When polymeric precursors were spin-coated five times on these films and then annealed again at 1000°C, it was expected that the thickness of the ZnO films would increase. It was found instead that the precursors settled among the islands of ZnO grains and did not increase the thickness significantly. FIB cross-section of Sample-2 does not show a distinct difference between the ZnAl<sub>2</sub>O<sub>4</sub> film and substrate. The thickness of the ZnO film is much lower than the c-sapphire substrate leading to a solid – state reaction leading to higher activation energy for the reactants [15]. On annealing a second time at 1000°C, the nucleation and growth rate increased faster to form ZnAl<sub>2</sub>O<sub>4</sub>, which is more stable than ZnO when Al<sub>2</sub>O<sub>3</sub> is greater than 1.45 weight % [22]. ZnAl<sub>2</sub>O<sub>4</sub> has been synthesized by the sol-gel method using Zn(NO<sub>3</sub>)<sub>2</sub> and Al(NO<sub>3</sub>)<sub>3</sub> as starting materials [23, 24]. However, in this work, ZnAl<sub>2</sub>O<sub>4</sub> has been synthesized due to interfacial reaction between the ZnO film and the sapphire substrate on annealing twice at 1000°C as in Sample-2.

#### **4. Conclusions**

Polymeric precursor derived ZnO thin films on sapphire substrates have been annealed at high temperatures to study the effect of annealing on thickness. Samples of single-layered and multilayered spin-coated ZnO films were annealed at 1000°C. XRD data of single-layered ZnO thin films (Sample-1) show that the synthesized films are polycrystalline with texturing along the (002) plane and have wurtzite structure with few ZnAl<sub>2</sub>O<sub>4</sub> peaks. However, XRD **pattern** of multilayered ZnO films, twice-annealed at 1000°C (Sample-2), show only ZnAl<sub>2</sub>O<sub>4</sub> peaks suggesting that ZnO reacted with the sapphire substrate. SEM micrographs illustrate that the ZnO films of Sample-1 are granular with shape ranging from spherical to polyhedral. Transmission spectra illustrate that Sample-1 has transparency (<50%) in the range 500–600 nm with the band edge at 376 nm, whereas the ZnO film of Sample-2 does not show any band edge. The single-layered ZnO film exhibits a strong UV emission PL peak at room temperature that is not shown by the multilayered ZnO film. The transmission and PL results confirm that there is absence of ZnO in the multilayered film, and that ZnO has reacted with the sapphire substrate to form ZnAl<sub>2</sub>O<sub>4</sub>. Hence, annealing twice at 1000°C, leads to the formation of ZnAl<sub>2</sub>O<sub>4</sub>, another wide band gap semiconductor.

#### **Acknowledgements**

The authors thank Dr. Richard Reidy and his group for their assistance in transmission measurements. They also thank Dr. Mohammed Omary and his group at the Department of Chemistry, University of North Texas, for their assistance in photoluminescence measurements.

## References

- [1] Y. Lare, A. Godoy, L. Cattin, K. Jondo, T. Abachi, F.R. Diaz, M. Morsli, K. Napo, M.A. del Valle, and J.C. Bernède, *Appl. Surf. Sci* 255 (2009) 6615.
- [2] T. Minemoto, T. Mizuta, H. Takakura, and Y. Hamakawa, *Sol. Energy Mater. Sol. Cells*. 91 (2007) 191.
- [3] S. Kishwar, K. ul Hasan, N.H. Alvi, P. Klason, O. Nur, and M. Willander, *Superlattice Microst.* 49 (2011) 32.
- [4] Q. Qiao, B.H. Li, C.X. Shan, J.S. Liu, J. Yu, X.H. Xie, Z.Z. Zhang, T.B. Ji, Y. Jia, and D.Z. Shen, *Mater. Lett.* 74 (2012) 104.
- [5] C. H. Ahn, D. K. Seo, C. H. Woo, and H. K. Cho, *Physica B* 404 (2009) 4835.
- [6] L. Cui, H. Y. Zhang, G. G. Wang, F. X. Yang, X. P. Kuang, R. Sun, and J. C. Han, *Appl. Surf. Sci* 258 (2012) 2479.
- [7] J. Lim, K. Shin, H. W. Kim, and C. Lee, *Mat. Sci. Eng. B* 107 (2004) 301.
- [8] Z. Zhao, L. Hu, H. Zhang, J. Sun, J. Bian, and J. Zhao, *Appl. Surf. Sci* 257 (2011) 5121.
- [9] K.-S. Hwang, B.-A. Kang, Y.-S. Kim, S. Hwangbo, and J.-T. Kim, *Ceram. Int.* 36 (2010) 2259.
- [10] B. Wessler, F. F. Lange and W. Mader, *J. Mater. Res.* 17 (2002) 1644.
- [11] U. Choppali and B. P. Gorman, *Mater. Chem. Phys.* 112 (2008) 916.
- [12] G. Du, J. Wang, X. Wang, X. Jiang, S. Yang, Y. Ma, W. Yan, D. Gao, X. Liu, H. Cao, J. Xu, and R.P.H. Chang, *Vacuum* 69 (2003) 473.

- [13] S.W. Xue, X.T. Zu, W.L. Zhou, H.X. Deng, X. Xiang, L. Zhang, and H. Deng, J. Alloys Compd 448 (2008) 21.
- [14] U. Choppali and B. P. Gorman, Opt. Mater. 31 (2008) 143.
- [15] Z. Bi, R. Zhang, X. Wang, S. Gu, B. Shen, Y. Shi, Z. Liu, and Y. Zheng, J. Am. Ceram. Soc. 86 (2003) 2059.
- [16] S. Uthanna, T.K. Subramanyam, B. S. Naidu, and G. M. Rao, Opt. Mater. 19 (2002) 461.
- [17] D. Visinescu, B. Jurca, A. Ianculescu, and O. Carp, Polyhedron 30 (2011) 2824.
- [18] R. T. Kumar, N. C. S. Selvam, C. Ragupathi, L. J. Kennedy, and J. J. Vijaya, Powder Technol. 224 (2012) 147.
- [19] S. T. Tan, X. W. Sun, X. H. Zhang , S. J. Chua, B. J. Chen, and C. C. Teo, J. Appl. Phys. 100 (2006) 033502.**
- [20] H.-G. Chen and Z.-W. Li, Appl. Surf. Sci. 258 (2011) 556.**
- [21] C. R. Gorla, W. E. Mayo, S. Liang, and Y. Lu, J. Appl. Phys. 87 (2000) 3736.**
- [22] E. W. Dewing, S. Rolseth, L. Stoen, and J. Thonstad, Metall. Mater. Trans. B 28B (1997) 1099.
- [23] X. Wei and D. Chen, Materials Lett. 60 (2006) 823.
- [24] F. Davar and M. Salavati-Niasari, J. Alloys Compd 509 (2011) 2487.

### Figure Captions

Figure 1: Flowchart depicting the procedure for preparation of the ZnO thin films.

Figure 2: Grazing incidence X-ray diffraction **pattern** of polymeric precursor based ZnO thin films (a) Sample-1 and (b) Sample-2. The **pattern** of Sample 2 shows only ZnAl<sub>2</sub>O<sub>4</sub> peaks.

Figure 3: In-plane X-ray diffraction **pattern** of annealed ZnO thin films of (a) Sample-1 and (b) Sample-2.

Figure 4: X-ray  $\phi$ -scan corresponding to the (101) ZnO reflection of Sample-1 annealed at 1000°C.

Figure 5: Low magnification SEM micrographs of the annealed ZnO thin films of (a) Sample-1 and (b) Sample-2; High magnification SEM micrographs of (c) Sample-1 and (d) Sample-2.

Figure 6: FESEM micrographs of FIB cross-section of precursor derived ZnO thin films (a) Sample-1 and (b) Sample-2.

Figure 7: Optical transmittance spectra of polymeric precursor derived ZnO thin films of (a) Sample-1 and (b) Sample-2.

Figure 8: Room temperature photoluminescence of ZnO thin films of (a) Sample 1 and (b) Sample-2.

Figure(1)  
[Click here to download high resolution image](#)

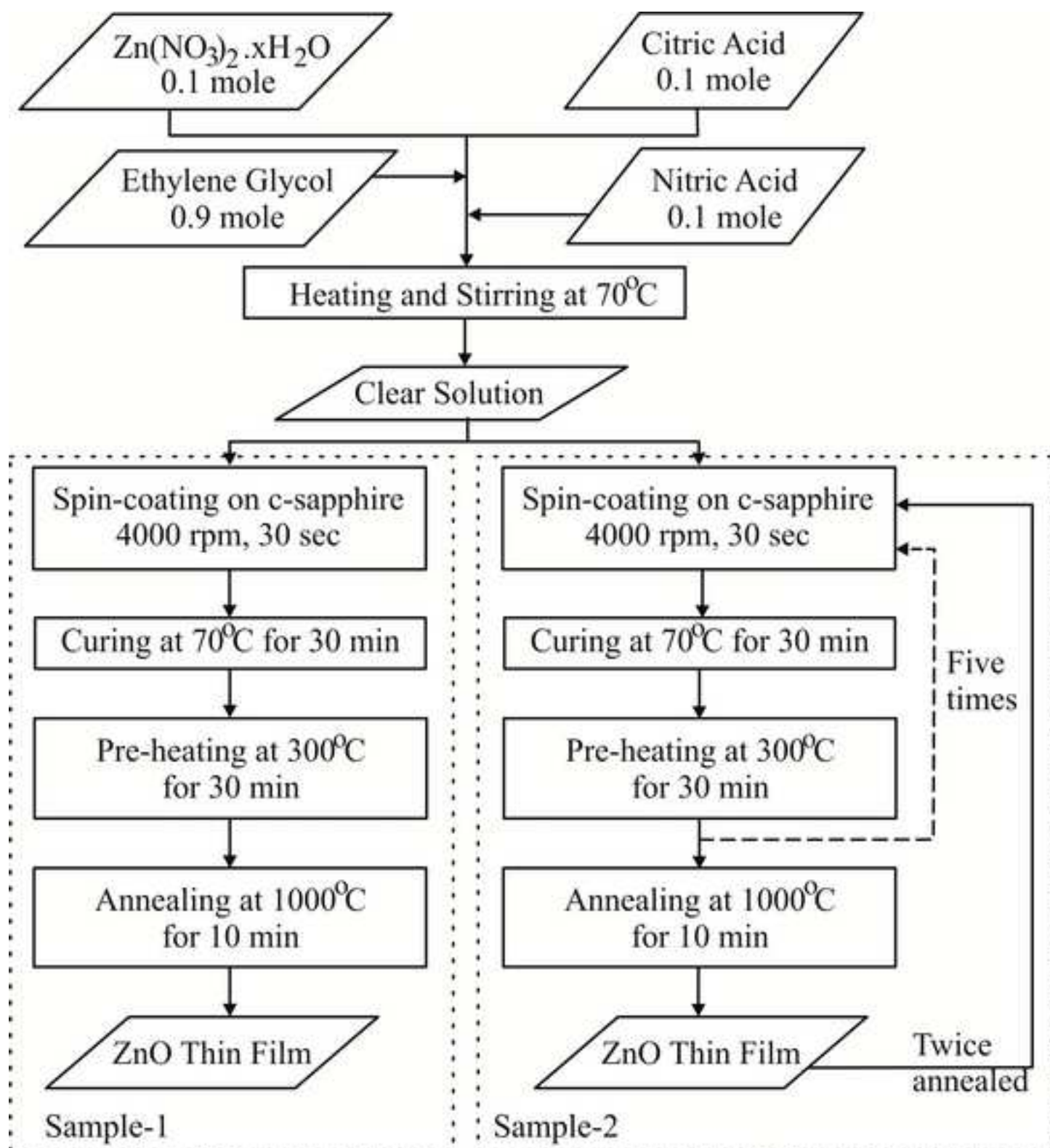


Figure 2

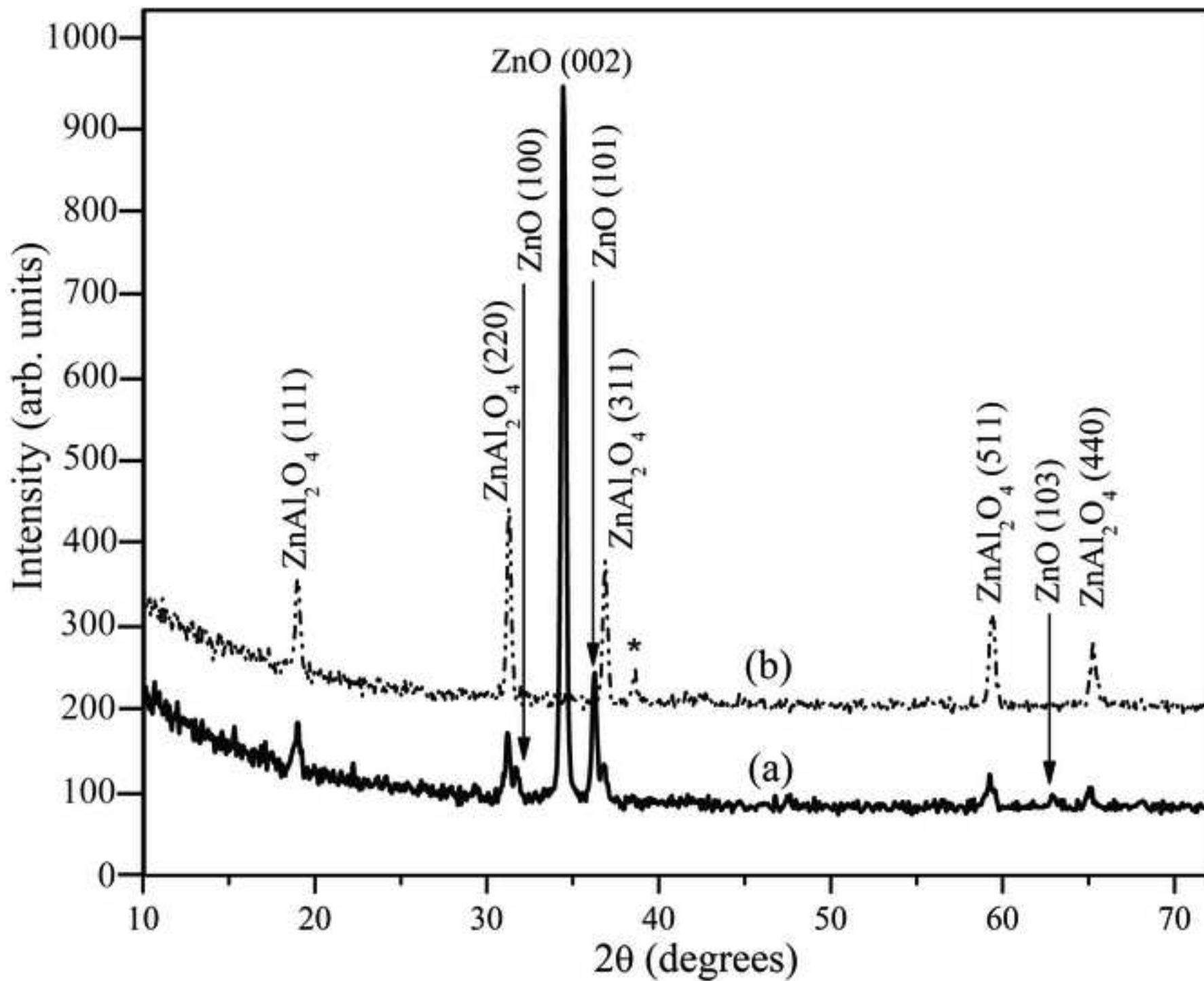
[Click here to download high resolution image](#)

Figure3  
[Click here to download high resolution image](#)

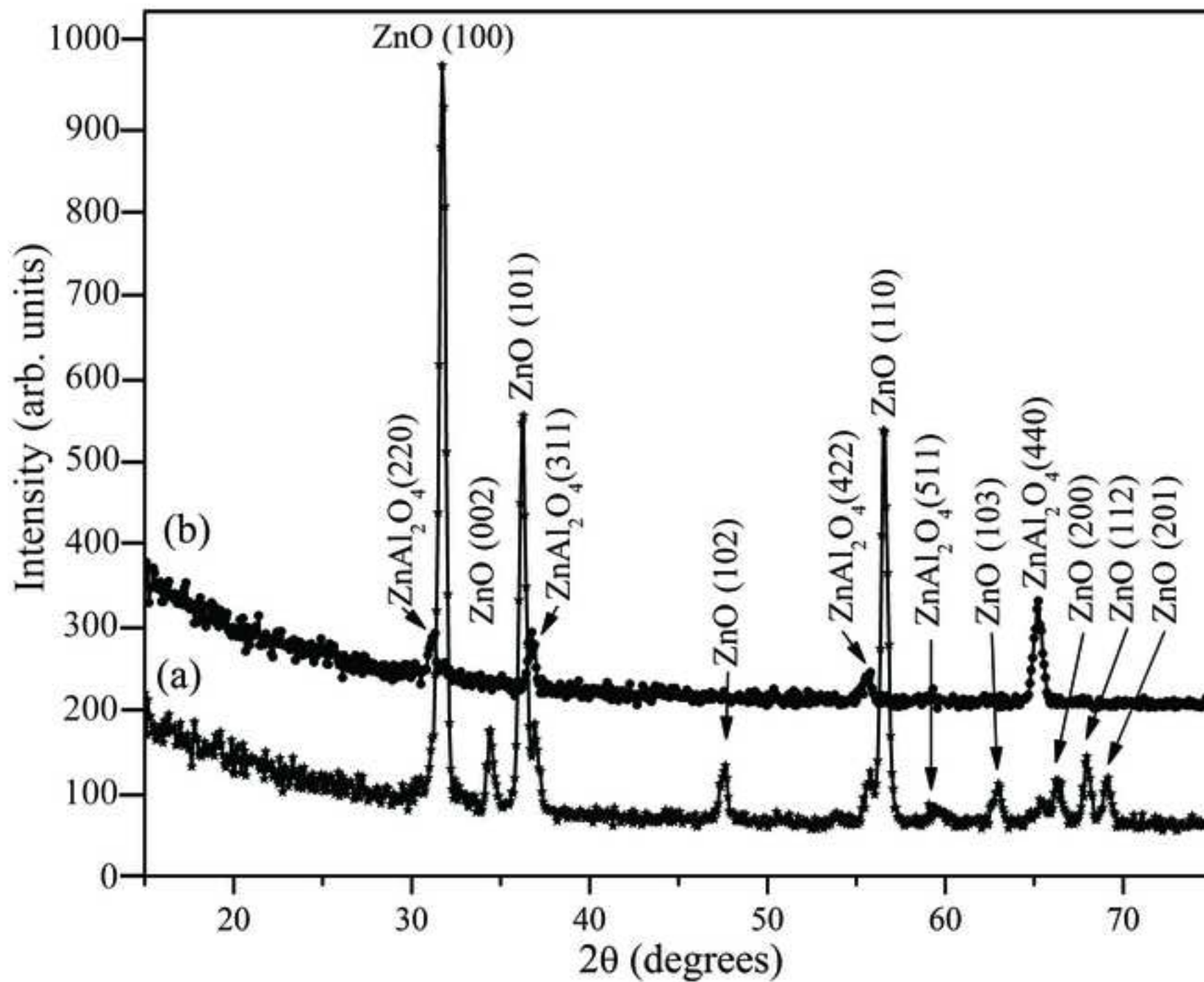
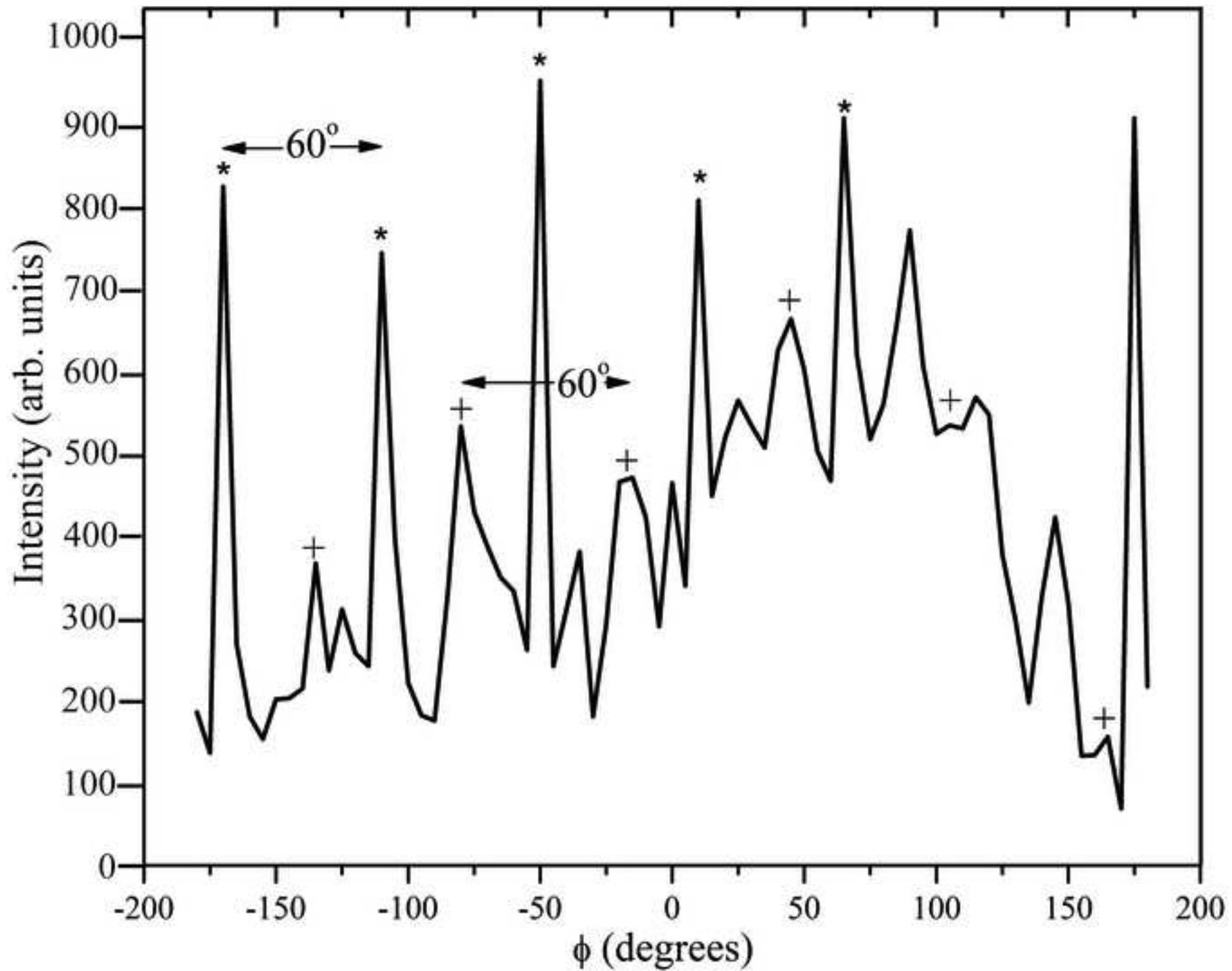


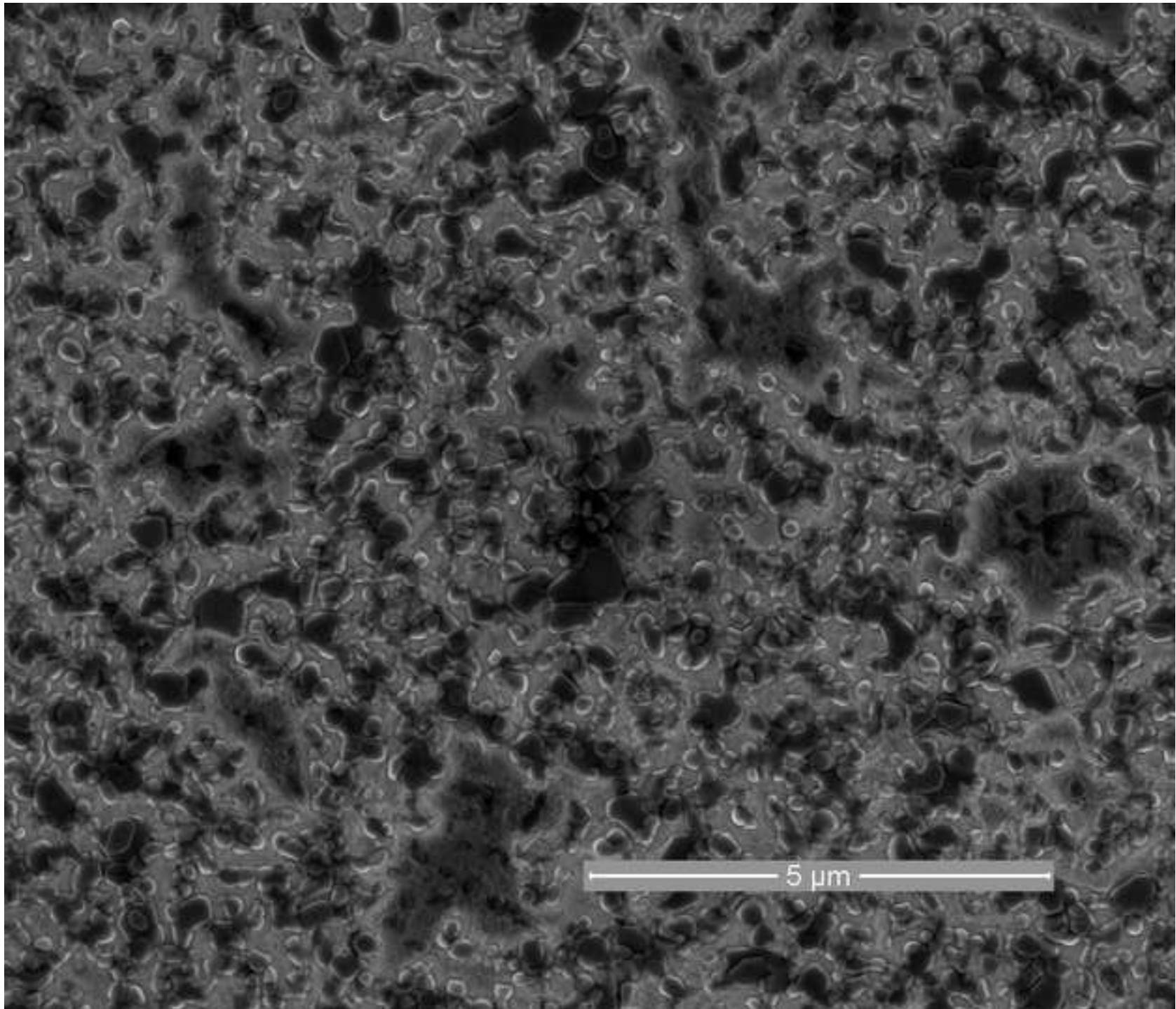
Figure4

[Click here to download high resolution image](#)



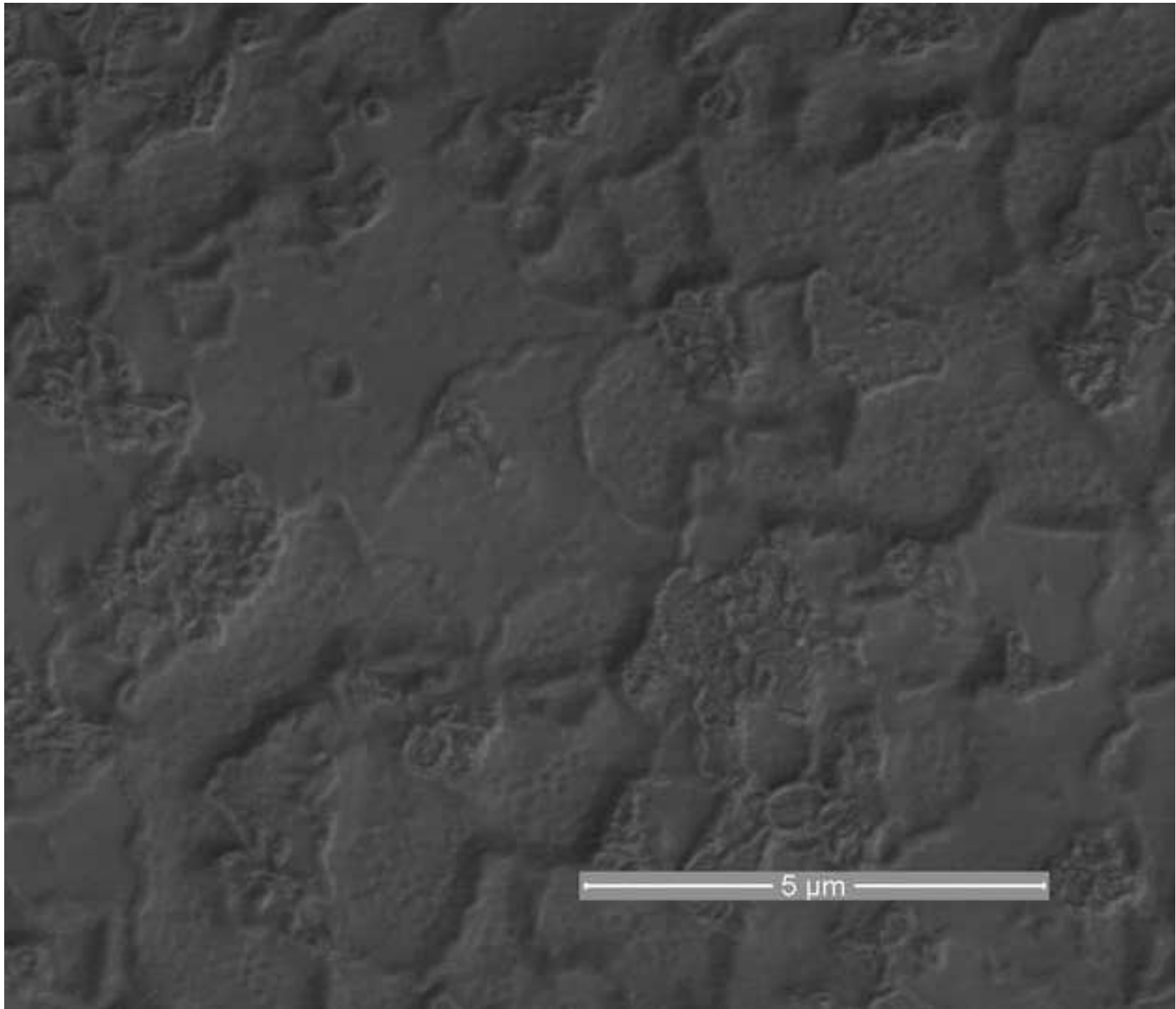
Figure(5a)

[Click here to download high resolution image](#)



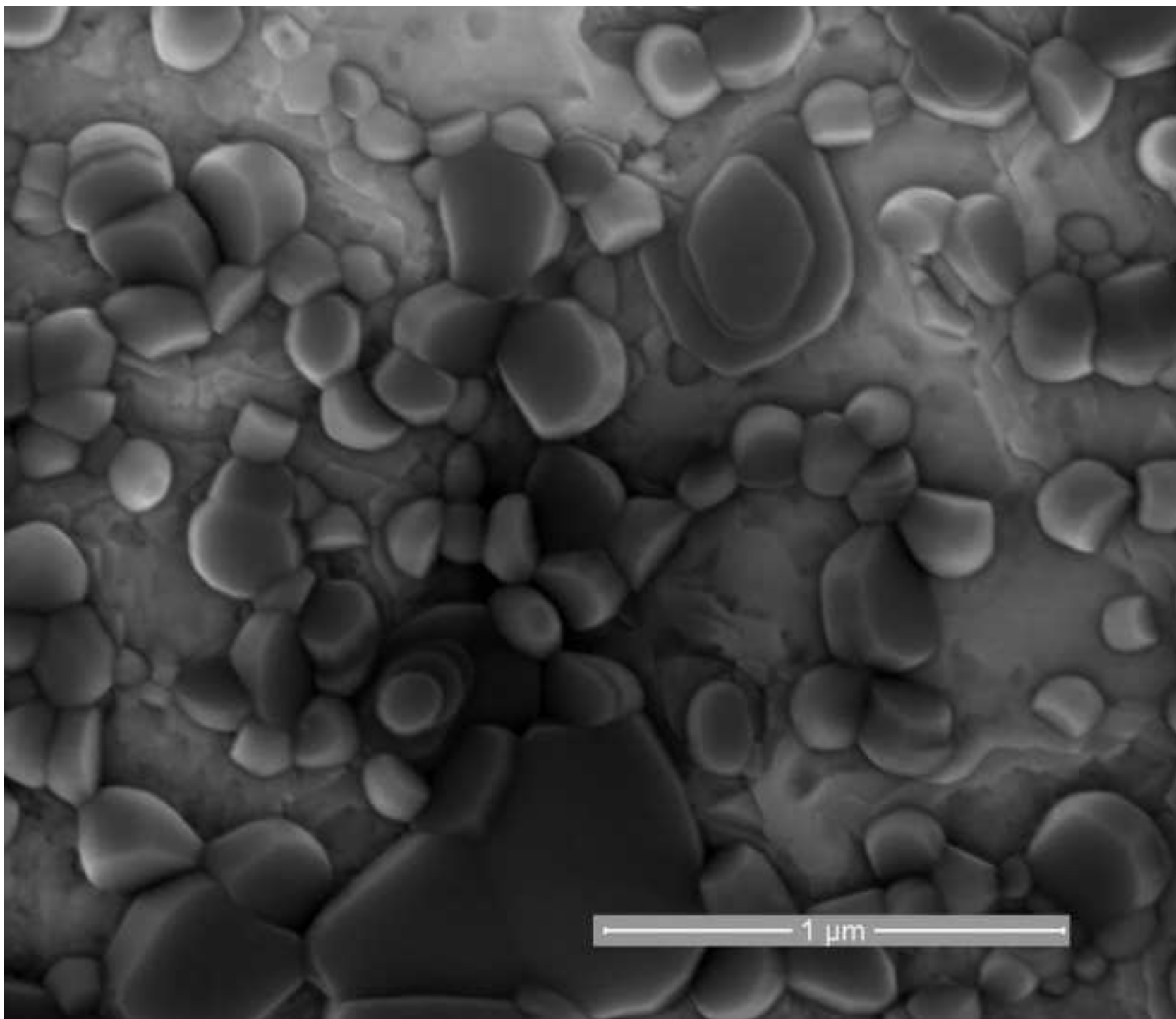
Figure(5b)

[Click here to download high resolution image](#)



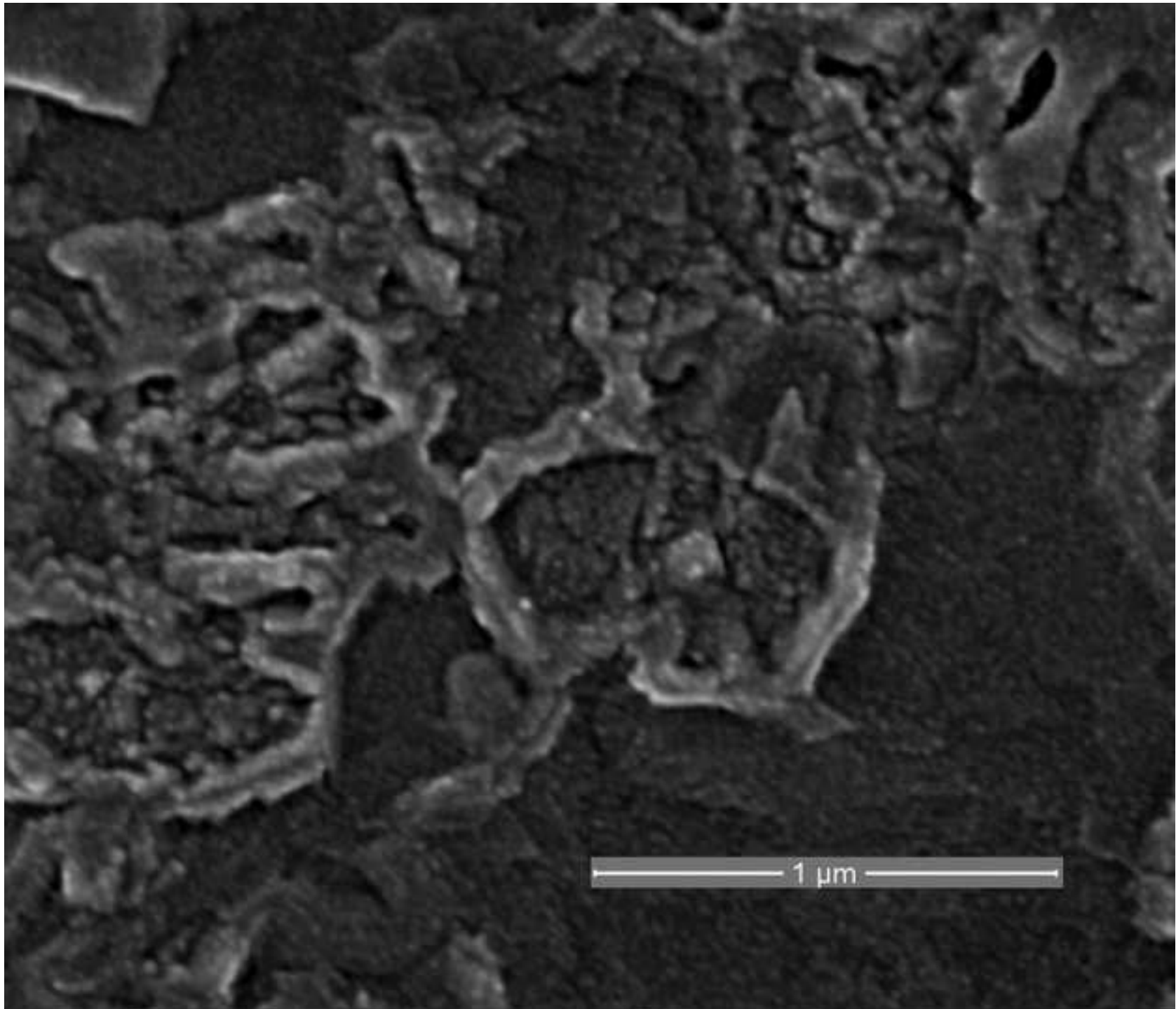
Figure(5c)

[Click here to download high resolution image](#)



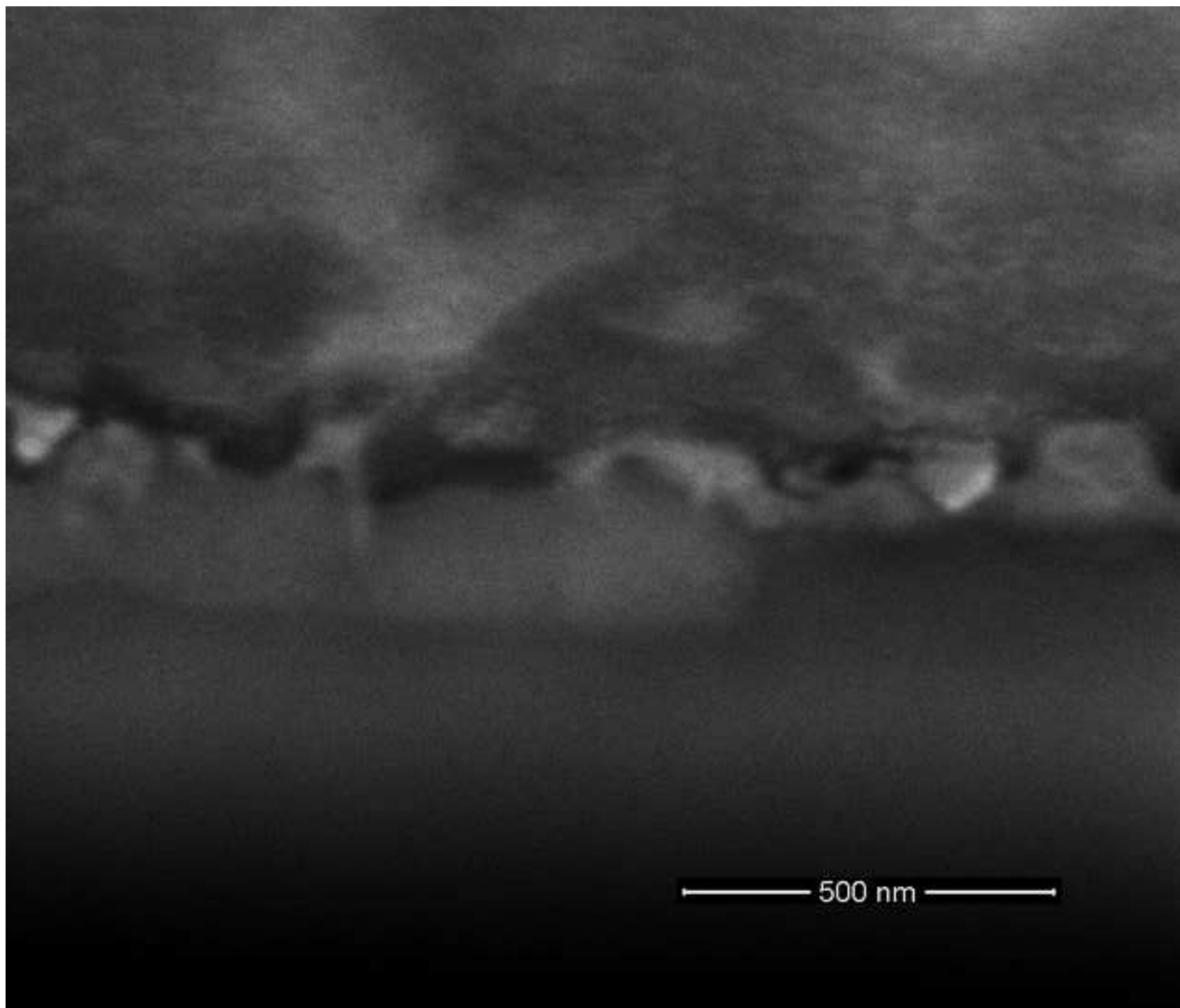
Figure(5d)

[Click here to download high resolution image](#)



Figure(6a)

[Click here to download high resolution image](#)



Figure(6b)

[Click here to download high resolution image](#)

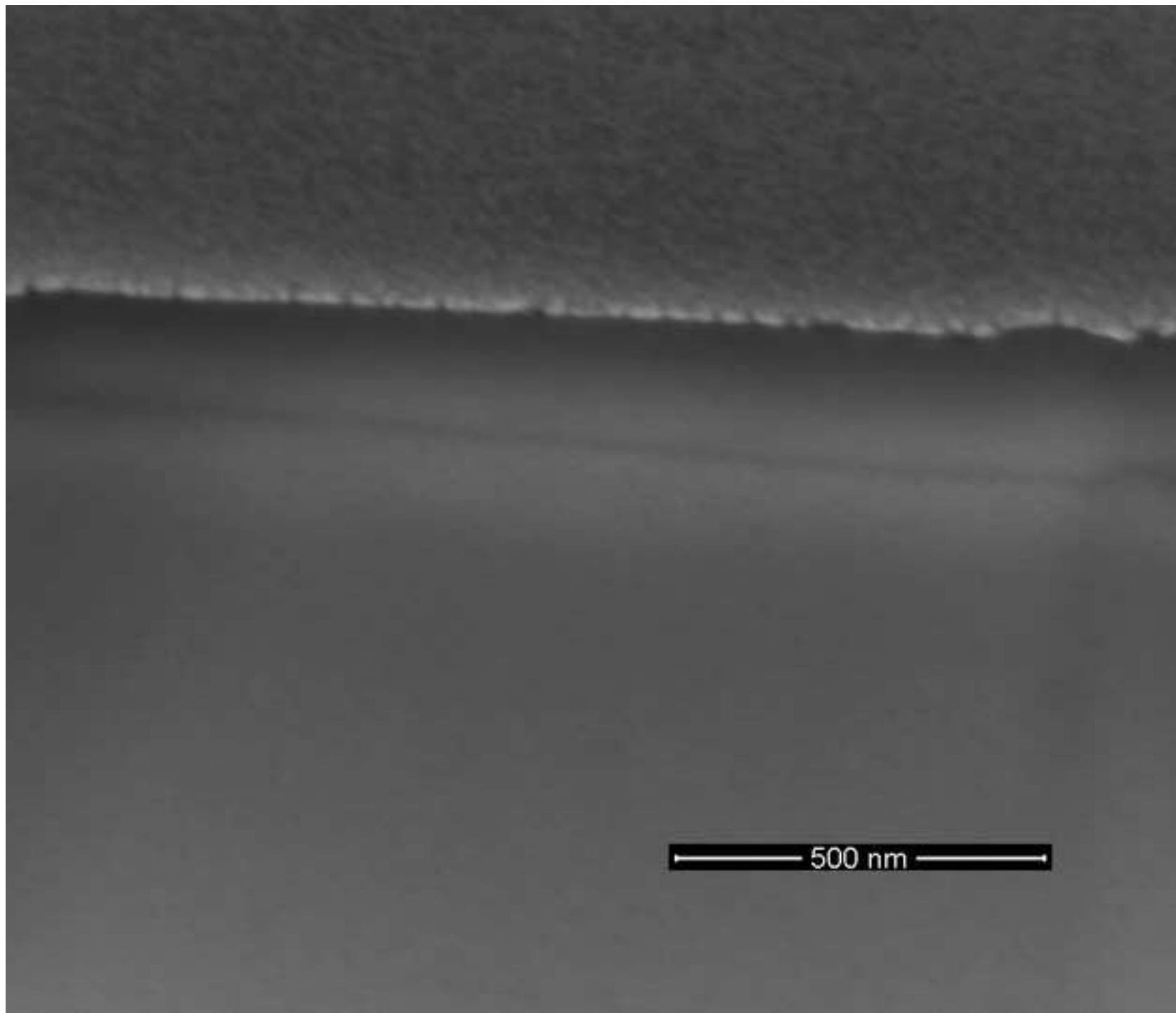


Figure7  
[Click here to download high resolution image](#)

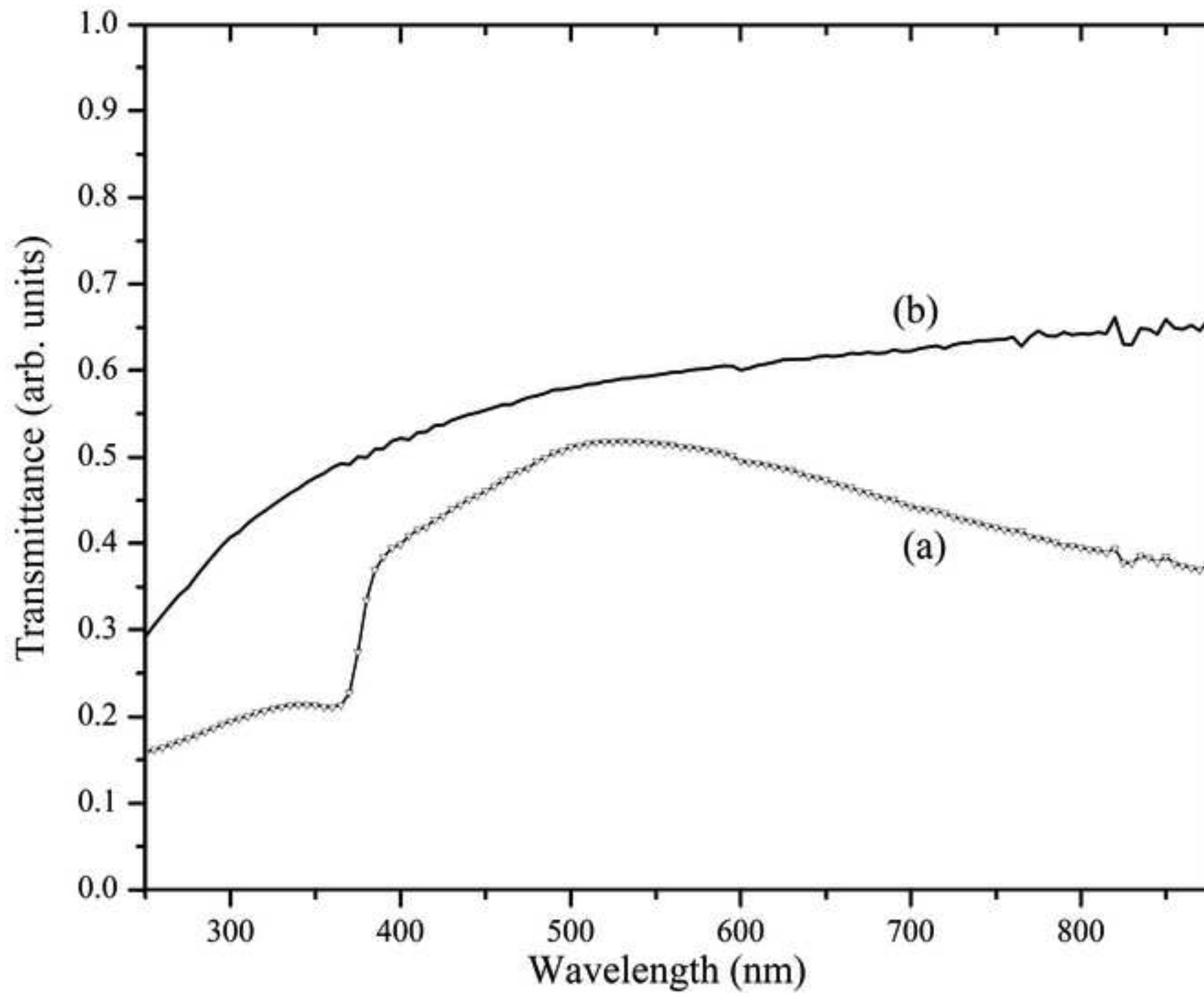


Figure8  
[Click here to download high resolution image](#)

